TOPICAL REVIEW — Magnetism, magnetic materials, and interdisciplinary research

Anomalous Hall effect in perpendicular CoFeB thin films*

Zhu Tao(朱 涛)†

Institute of Physics and Beijing National Laboratory for Condensed Matter Physics, Chinese Academy of Sciences, Beijing 100190, *China*

(Received 18 February 2014; published online 20 March 2014)

Our recent research achievements in the perpendicular magnetic anisotropy (PMA) properties of the CoFeB sandwiched by MgO and tantalum layers are summarized. We found that the PMA behaviors of Ta/CoFeB/MgO and MgO/CoFeB/Ta thin films are different. The larger PMA in the latter film is related to the lower magnetization of CoFeB deposited on MgO. Furthermore, we have demonstrated a large anomalous Hall effect in perpendicular CoFeB thin film. Our results show large anomalous Hall resistivity, large longitudinal resistivity, and low switching field can be achieved, all at the same time, in the perpendicular CoFeB thin film. Anomalous Hall effect with high and linear sensitivity is also found in an MgO/CoFeB/Ta thin film with a thick MgO layer, which opens a door for future device applications of perpendicular ferromagnetic thin films.

Keywords: anomalous Hall effect, perpendicular magnetic anisotropy, magnetic properties of interfaces

PACS: 75.47.–m, 75.30.Gw, 75.70.Cn, 75.25.+z **DOI:** 10.1088/1674-1056/23/4/047504

1. Introduction

Magnetic anisotropy has been investigated for decades.[1] For example, a perpendicular magnetic thin film has been widely used in high density storage media.[2] A magnetic tunnel junction with a perpendicular magnetic anisotropy (PMA) enables a small critical current density for current-induced magnetization switching.[3] Understanding magnetic anisotropy is one of the keys for the applications of the ferromagnetic thin films. Several candidate materials exhibit PMA, such as Co/Pt and Co/Ni multilayers,[3,4] CoFeB/Pd bilayers,[5] FePt single layers,[6] and so on. Recently, Ikeda *et al.* reported observing PMA in a CoFeB layer sandwiched by MgO and Ta layers,[7] which has potential applications in spin transfer torque devices.[7] Although the PMA is believed to arise from the interfacial anisotropy at the MgO/CoFeB interface,[8] the origin of the PMA remains elusive. Worledge *et al.* pointed out that the Ta/CoFeB interface plays a key role in making the CoFeB magnetization perpendicular.[9] Most recently, by employing polarized neutron reflectometry (PNR), we observed a robust difference in magnetization in the CoFeB layer, depending on whether it is above or below an MgO layer,[10] indicating that a large PMA is related to the low magnetization of CoFeB deposited on MgO.

Magnetic hysteresis measurement is a direct method for studying PMA in a magnetic thin film. Anomalous Hall effect (AHE) is also widely used to characterize perpendicular magnetic films.[11] Figure 1 shows the Hall bar geometry. In principle, Hall resistivity (ρ_{xy}) in a ferromagnet is defined as[12]

$$\rho_{xy} = R_0 H + \mu_0 R_S M_\perp, \tag{1}$$

where ordinary Hall resistivity $R_0 H$ is proportional to the induced field H, whereas anomalous Hall resistivity $\mu_0 R_S M_\perp$ is proportional to the magnetization along the perpendicular direction $M_\perp$. R_0 and R_S are Hall constants for ordinary and anomalous Hall effects, respectively. Anomalous Hall resistivity ρ_{AH} is then determined by extrapolating the magnetically saturated state back to zero field, which characterizes the anomalous Hall effect of materials.

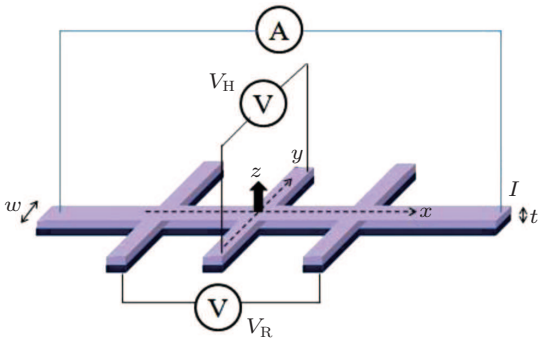


Fig. 1. The Hall bar geometry for measurement.

Indeed, AHE itself has continually gained much interest as a fundamental property of the magnetic solids. PMA can induce a highly sensitive anomalous Hall effect in a perpendicular ferromagnetic thin film, making it a candidate for a magnetic field sensor or a logic device for spintronics applications.[12–17] Most recently, we have demonstrated

*Project supported by the National Basic Research Program of China (Grant No. 2012CB933102) and the National Natural Science Foundation of China (Grant Nos. 50871120, 11079052, and 11174354).

†Corresponding author. E-mail: tzhu@iphy.ac.cn

© 2014 Chinese Physical Society and IOP Publishing Ltd

a large anomalous Hall effect in the perpendicular CoFeB thin film. In this paper, we present recent progress in the perpendicular CoFeB thin films. It is organized as follows. Section 2 provides details about recent advances in the perpendicular CoFeB thin films. Section 3 describes the AHE properties of the perpendicular CoFeB thin films. Section 4 is a preliminary summary of proposed AHE mechanisms for the perpendicular CoFeB thin films. Applications of the AHE that exists in the perpendicular CoFeB thin films are discussed in Section 5. Finally, the conclusions of all this work are summarized in Section 6.

2. Perpendicular magnetic anisotropy in CoFeB sandwiched by MgO and tantalum layers

In the initial work, Yakata *et al.* found that PMA is induced at the MgO barrier–Fe-rich CoFeB interface.[18] And then Ikeda *et al.* reported finding PMA in a thin CoFeB layer (< 1.5 nm) sandwiched by MgO and Ta layers.[7] One of the pathways to achieve higher stability of the memory cells is to enhance the PMA further. For example, Kubota *et al.* reported the use of FeB in place of CoFeB.[19] Nevertheless, the investigation of the origin of PMA in perpendicular CoFeB thin films is necessary.[7–10,18–20] In a CoFeB sandwiched by MgO and tantalum layers, the effective magnetic anisotropy in first order approximation can be generally defined as[20]

$$K_{\rm eff} = \left(K_{\rm b} - \frac{1}{2}\mu_0 M_{\rm S}^2\right) + K_{\rm S,MgO/CoFeB}/t_{\rm CoFeB}, \qquad (2)$$

where $t_{\rm CoFeB}$ is the CoFeB thickness and $M_{\rm S}$ is the saturation magnetization of the CoFeB layer. $K_{\rm b}$ is the bulk crystalline anisotropy, which can be neglected.[7] The perpendicular anisotropy in a ferromagnetic film is the result of the competition between the demagnetization energy ($\frac{1}{2}\mu_0 M_{\rm S}^2$) and the interfacial anisotropy energy ($K_{\rm S}/t_{\rm CoFeB}$). The interfacial anisotropy energy sensitively depends on the interface structure. A perpendicular easy axis of magnetization is obtained when $K_{\rm eff} > 0$.

To study the details of perpendicular magnetic anisotropy properties in perpendicular CoFeB thin films, two series of samples, MgO(1.1)/$Co_{40}Fe_{40}B_{20}$(1.22)/Ta[0.55–4.4] and Ta(2.2)/$Co_{40}Fe_{40}B_{20}$(1.04)/MgO[0.44–5.5], hereinafter defined as MgO/CoFeB/Ta and Ta/CoFeB/MgO, respectively, were deposited on thermally oxidized silicon substrates (Si/SiO_2) by magnetron sputtering with a base pressure of 4×10^{-6} Pa. The numbers in brackets are nominal thicknesses in nanometers. The samples with a Hall bar were then annealed at a temperature $T_{\rm ann}$ ranging from 120 °C to 400 °C in a vacuum for an hour. Argon was used as the sputtering gas, and the sputtering pressure for metals was 0.4 Pa. MgO layers were deposited by radio frequency sputtering, and the sputtering pressure was 0.2 Pa. Room-temperature anomalous Hall resistance loops (R_{xy}–H) were measured in a commercial Hall probing system with an electromagnet at up to 1.5 T to characterize the PMA property. The magnetoresistance in all the films at 1.5 T is smaller than 0.2%.

Figure 2(e) shows the out-of-plane squareness ($R_{xy}^{\rm r}/R_{\rm AH}$) and the coercivity field ($H_{\rm C}$) as functions of the thickness of the tantalum cap layer for a series of tantalum capping films (MgO/CoFeB/Ta) annealed at $T_{\rm ann} = 300$ °C. Here, $R_{xy}^{\rm r}$ is the remnant Hall resistance at $H = 0$. The films show the in-plane magnetic easy axis when $t_{\rm Ta} < 0.55$ nm, suggesting that the CoFeB/MgO interface alone cannot provide a large enough interfacial anisotropy to induce the out-of-plane anisotropy in the CoFeB layer. The out-of-plane squareness increases with the tantalum cap layer thickness from 0.55 nm to 0.94 nm and reaches the maximum value of 1 at $t_{\rm Ta} = 0.94$ nm. Unity squareness ($R_{xy}^{\rm r}/R_{\rm AH} = 1$) can be observed at the tantalum cap layer thickness at up to 4.4 nm, although the out-of-plane coercivity decreases to $H_{\rm C} = 4.14$ kA/m.

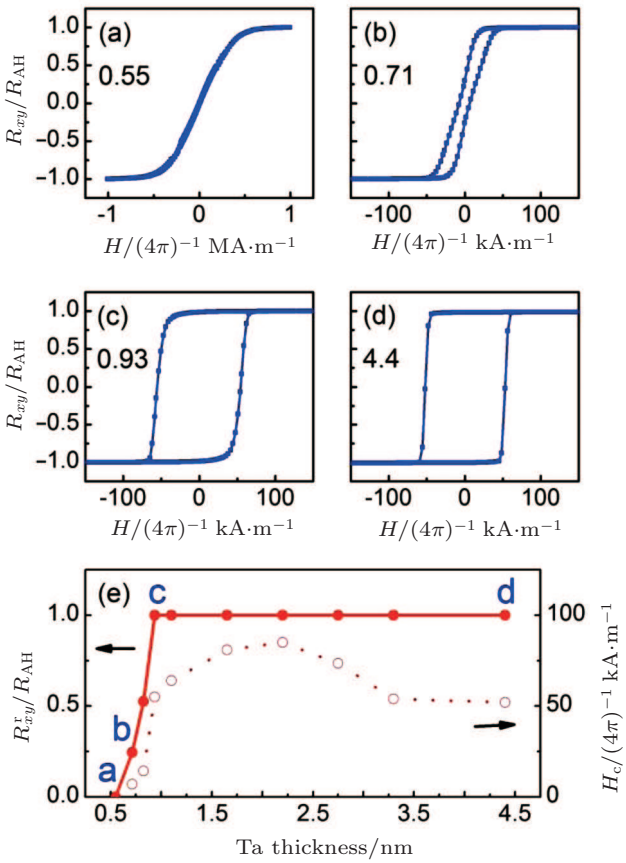


Fig. 2. Representative curves of R_{xy} versus H for annealed MgO(1.1)/CoFeB(1.22)/Ta(t) films ($T_{\rm ann} = 300$ °C) with $t_{\rm Ta}$ = (a) 0.55, (b) 0.71, (c) 0.94, and (d) 4.4 nm, denoted by the letters in the bottom panel. (e) Tantalum cap layer thickness dependencies of the out-of-plane $R_{xy}^{\rm r}/R_{\rm AH}$ (open circles) and $H_{\rm C}$ (solid circles).

We also investigated the dependence of $R_{xy}^{\rm r}/R_{\rm AH}$ and $H_{\rm C}$ on the thickness of the MgO capping layer for a series of tantalum capping films (Ta/CoFeB/MgO) annealed at $T_{\rm ann} = 300$ °C.[21] Figure 3 shows the $R_{xy}^{\rm r}/R_{\rm AH}$ and $H_{\rm C}$ as

functions of the thickness of the MgO cap layer. The films show a magnetic easy axis in the plane when t_{MgO} <0.77 nm, whereas PMA and unity squareness ($R^{r}_{xy}/R_{AH} = 1$) were observed when $t_{MgO} < 0.77$ nm. This is to say, CoFeB has perpendicular anisotropy when it sandwiched by Ta and MgO layers. It is also surprising that the strength of the perpendicular anisotropy is dependent on the stack deposition sequence.

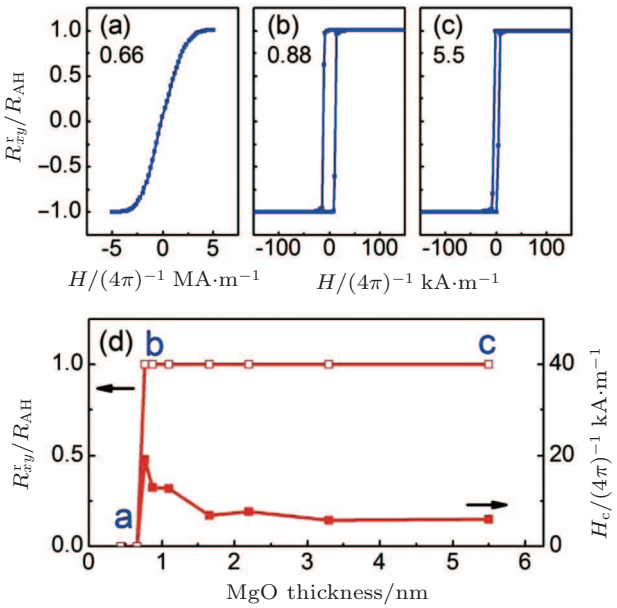


Fig. 3. Representative curves of R_{xy} versus H for annealed Ta (2.2)/CoFeB(1.22)/ MgO(t) films ($T_{ann} = 300$ °C) with t_{MgO} = (a) 0.66, (b) 0.88, and (c) 5.5 nm, denoted by the letters in the bottom panel. (d) MgO cap layer thickness dependencies of the out-of-plane R^{r}_{xy}/R_{AH} (open circles) and H_C (solid circles).

In order to study the origin of PMA further and to explain the stack-deposition sequence-dependent PMA, the polarized neutron reflectometry (PNR) technique was utilized to directly measure the individual magnetization in the stacks. PNR measurements were carried out by using the Magnetism Reflectometer (BL-4A) at SNS.[22] The two non-spin-flip (NSF) cross sections (R^{++} and R^{--}) are measured as a function of scattering vector Q. The sample's depth-dependent nuclear scattering length density $\rho_N(z)$ and the magnetic scattering density $\rho_M(z)$ (which is a measure of the projection of the magnetization along the applied field direction) are determined by fitting the NSF data. The sample for PNR measurement was prepared as an MTJ-like structure, i.e., Ta(2.2)/CoFeB(1.04)/MgO(1.1)/CoFeB(1.22)/Ta(2.2) on Si/SiO_2 (T_a = 300 °C). This MTJ-like structure combined two types of PMA thin films: MgO/CoFeB/Ta and Ta/CoFeB/MgO. In principle, PNR is a technique that is sensitive to the compositional and in-plane magnetic depth profiles of thin films, but not sensitive to layer magnetization perpendicular to the sample surface.[23] Therefore, a large in-plane field is applied to saturate the out-of-plane magnetization into the hard in-plane direction. Figure 4 shows the measured room temperature polarized neutron reflectivity data in $H = 1$ T. This PNR experiment was the first to demonstrate a robust difference in magnetization between CoFeB layers, depending on whether they are above or below an MgO layer.[10] A large PMA in MgO/CoFeB/Ta thin film is related to the low magnetization of CoFeB deposited on MgO.

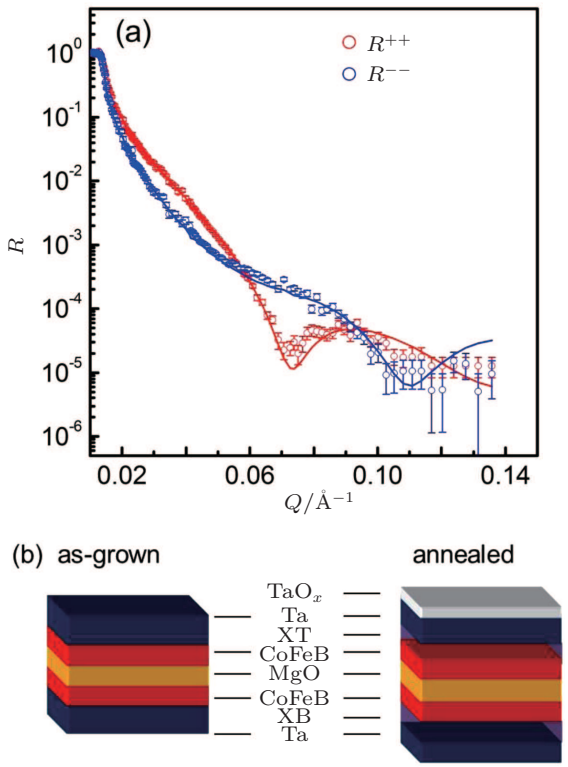


Fig. 4. Experimental PNR data taken at room temperature in $H = 1$ T. Solid lines are the fitted data. Right panel shows the stack structure of the PNR sample obtained from nuclear scattering length density profiles. X is the interfacial layer between CoFeB and Ta.

According to Eq. (2), the demagnetization term ($\frac{1}{2}\mu_0 M_S^2$) plays a key role in inducing PMA in a ferromagnetic thin film. The effective perpendicular anisotropy in a perpendicular film is often determined by[24]

$$K_{eff} = \frac{\mu_0 H_K M_S}{2}. \quad (3)$$

To take into account the absolute magnetization $M_S = 9.06 \times 10^5$ A/m and $H_K = 4.3 \times 10^4$ A/m for Ta(2.2)/CoFeB(1.04)/MgO(1.1), K_{eff} is calculated as 2.4×10^4 J/m, which is quite close to results reported by Yamanouchi *et al.*[20] However, K_{eff} is calculated as 4×10^4 J/m for MgO(1.1)/CoFeB(1.22)/Ta(2.2), where $M_S = 6.63 \times 10^5$ A/m and the $H_K = 9.7 \times 10^5$ A/m. The K_{eff} of the tantalum capping film is about 66% larger than that of the MgO capping film.[10] Consequently, PMA is strongly dependent on the stack deposition sequence.

In conventional ferromagnetic metal/non-magnetic (FM/NM) metal multilayers, the interfacial anisotropy arises due to spin–orbit interaction (SOI) at the interface.[25] Interfaces between magnetic and heavy nonmagnetic metals such

as Co/Pt, Co/Pd, and Co/Au have been used to obtain PMA. It has been shown that the onset of PMA at these interfaces is related to an increase in the orbital momentum of Co due to the strong hybridization between the 3d orbitals of the transition metal and the 5d orbitals of the heavy metal. As for the perpendicular Pt/Co/AlOx thin film,[11] the strong PMA has been confirmed at interfaces between magnetic transition metals and oxygen-terminated oxides.

In accord with the previous calculation of Fe/MgO,[26] the origin of the large PMA at the interface of FM and oxide is ascribed to a combination of several factors: the lifting of the degeneracy of out-of-plane 3d orbitals (d_{xz} and d_{yz}), hybridizations between d_{z2} and $d_{xz(yz)}$ induced by SOI, and hybridizations between Fe-3d and O-2p orbitals at the interface between the transition metal and the insulator. Here, the hybridization between d_{z2} and p_z is not split. On the other hand, SOI lifts the degeneracy for the states d_{xzyz} causing the split of the out-of-plane magnetization orientation to be more pronounced than the in-plane split, and resulting in larger PMA. Recently, we finished the *ab initio* calculation of the PMA for the CoFeB/MgO interface.[27] Figure 5 shows the supercell for the *ab initio* simulation of the Fe and MgO interface. Fe, Co, Mg, and O were represented by yellow, blue, green, and red balls, respectively. PMA at CoFe(B)/MgO interfaces is believed to originate from the hybridization of Fe-3d and O-2p orbitals, which is strongly determined by the structure of the CoFe(B)/MgO interface. Then the redistribution of O vacancies plays an essential role in PMA at the CoFeB/MgO interface.

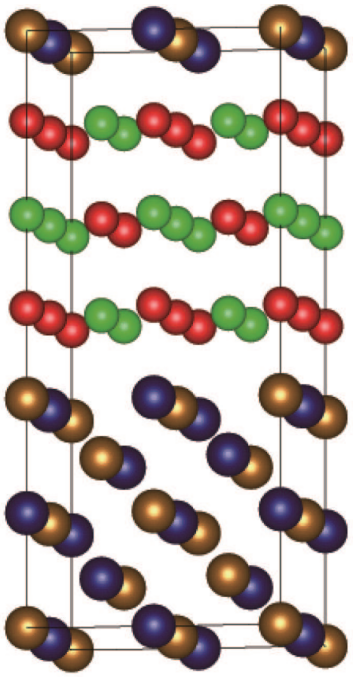


Fig. 5. Supercell for the *ab initio* simulation of the Fe and MgO interface. Fe, Co, Mg, and O are represented by yellow, blue, green, and red balls, respectively.

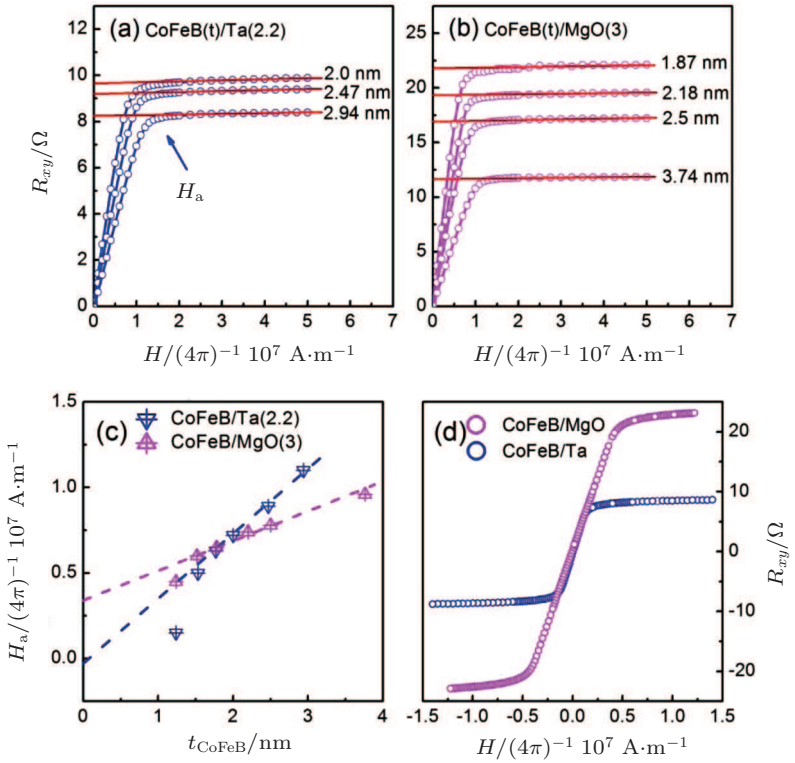


Fig. 6. R_{xy} curves as functions of the applied field H for annealed ($T_{ann} = 300$ °C) (a) CoFeB/Ta and (b) CoFeB/MgO bilayers with different CoFeB layer thickness. (c) The CoFeB thickness dependence of the out-of-plane saturation field, H_a. (d) R_{xy} curves as functions of the applied field H for annealed CoFeB/Ta and CoFeB/MgO bilayers with $t_{CoFeB} = 1.24$ nm.

Indeed, there are two interfaces, that is, CoFeB/Ta and MgO/CoFeB. To further clarify the origin of PMA in CoFeB sandwiched by Ta and MgO layers, we measured these two kinds of interfaces (CoFeB/Ta and CoFeB/MgO on SiO_2/Si). Figure 6 shows R_{xy}–H curves. It also shows the out-of-plane saturation field (H_a), which decreases for both bilayers with decreasing thickness of CoFeB. Compared with the perpendicular CoFeB sandwiched by Ta and MgO layers, both CoFeB/Ta and CoFeB/MgO bilayers ($t_{CoFeB} = 1.2$ nm) show in-plane easy axes. This is to say that neither CoFeB/Ta nor CoFeB/MgO bilayer can exhibit PMA. As mentioned above in PNR measurements, we unambiguously determined the depth profile of the boron distribution and showed that after annealing, most of the boron diffused to form a 2-nm-thick interface layer between the CoFeB and tantalum layers, using the sensitivity of neutrons to the absorption cross section of boron. The observation of the thick interface between Ta and CoFeB indirectly confirms that the MgO/CoFe(B) interface may mainly induce the large PMA in MgO/CoFeB/Ta or Ta/CoFeB/MgO thin films. The purpose of Ta may be the layer to absorb B out of the CoFeB layer.

Furthermore, it is also found that there is negligible PMA at $t_{Ta} < 0.55$ nm because CoFeB cannot be avoided for oxidation with such a thin capping layer (see Fig. 2). A clear PMA with $R^r_{xy}/R_{AH} = 1$ is obtained when the nominal tantalum thickness is above 0.94 nm, but no strong relationship between PMA and the thickness of the thick Ta cap layer. The Ta cap layer alone is sufficient to ensure the chemical stability of a general spintronics sample over time because of the formation of a dense tantalum oxide. As was found previously, a 1-nm-thick Ta layer can completely protect the samples.[28] Hence, further increasing the Ta thickness ($t_{Ta} > 2$ nm) has little effect on the interface and is not expected to change the PMA.

3. Anomalous Hall effect of perpendicular CoFeB thin film

AHE is a fundamental property of the magnetic solids, and as such, has continually attracted growing interest. The investigation of PMA properties using AHE is just an example. As for AHE itself, the research has focused on alloys or multilayers involving a noble metal, such as Pt. In these materials, strong spin–orbit interactions are induced.[13,14] Typical Hall angles of Pt-based multilayer are in the range of 1%–3%, but ρ_{xx} (∼ several tens μΩ·cm) are suppressed by thick Pt layers, which limits the desired reduction of device sizes.[29] Ferromagnetic metal–insulator granular films also have high ρ_{xx} when the proportion of the metal (by volume) is below a critical value (x_C). A giant AHE has been reported in the Ni–SiO_2 granular film,[30] but its Hall angle is unfortunately low (0.1%). So far, no material can satisfy the applications' requirements for large anomalous Hall resistivity, large longitudinal resistivity, and low switching field, all at the same time.[29] In this section, we demonstrate a large AHE in the perpendicular CoFeB thin film, in which simultaneous large ρ_{AHE}, large ρ_{xx}, and low switching field are quite possible.

Figure 7 shows CoFeB thickness dependence of ρ_{AHE} and ρ_{xx} for annealed MgO (1.1)/CoFeB (t)/Ta (2.2) films ($T_{ann} = 300$ °C).[31] The numbers in brackets are nominal thicknesses in nanometers. The insets show the representative Hall resistance hysteresis loops ($R_{xy}H$) with t_{CoFeB}. Similar with previous results,[7–10] obvious perpendicular magnetic anisotropy has been obtained when CoFeB thickness ranging from 1.06 nm to 1.5 nm in the Ta capping films. As shown in Fig. 7, the ρ_{AHE} values are significantly larger than those of ordinary transition metals (∼ 1 μΩ·cm[12]). From a simple view, it is well known that large AHE arises from the strong spin–orbit coupling.[13,14] Similar Pt, Ta also has a strong spin–orbit interaction because it is the heavy nonmagnetic metal. With a decrease of CoFeB thickness, a significantly large ρ_{AHE} of the perpendicular CoFeB is retained. Here, we calculate ρ_{AHE} and ρ_{xx} by subtracting an experimental value of 0.45 nm from the nominal thickness of Ta due to the oxidation of Ta on the top of samples (see below).

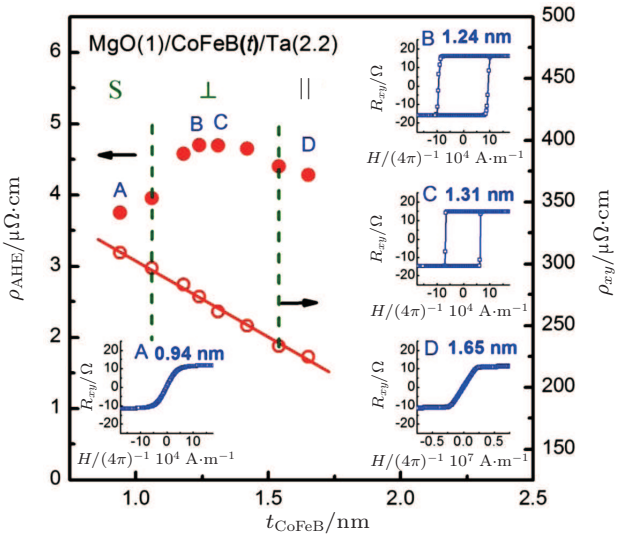


Fig. 7. CoFeB thickness dependence of ρ_{AH} and ρ_{xx} for annealed MgO (1.1)/CoFeB (t)/Ta (2.2) films ($T_{ann} = 300$ °C) with S defined as superparamagnetic, ⊥ as magnetic easy axis perpendicular to film, and || as magnetic easy axis in the plane. The insets show the representative curves of R_{xy} versus H with t_{CoFeB} (denoted by the letters).

Another pronounced feature in Fig. 7 is the large longitudinal resistivity of the samples. Indeed, the ρ_{xx} of all the samples of CoFeB sandwiched by MgO and Ta layers is larger than 100 μΩ·cm and increases with a decrease of CoFeB thickness; this ρ_{xx} is several times larger than that of the traditional Pt-based multilayers and alloys. Figure 8 shows a typical curve

for the temperature dependence of $\rho_{\rm AHE}$ versus ρ_{xx}. The ρ_{xx} increases with decreasing temperature. Similar negative temperature coefficient has reported in the temperature dependence of the longitudinal resistivity for some amorphous materials. Note that bulk resistivity of Ta is about 200 μΩ·cm[32] due to its extremely short mean free path (∼ 1 nm). Hence, the large resistivity found in samples comes from the high resistivities of both the Ta and CoFeB (about 160 μΩ·cm[33]) layers — a characteristic believed to be a key to reducing the size of devices in practical applications.[29]

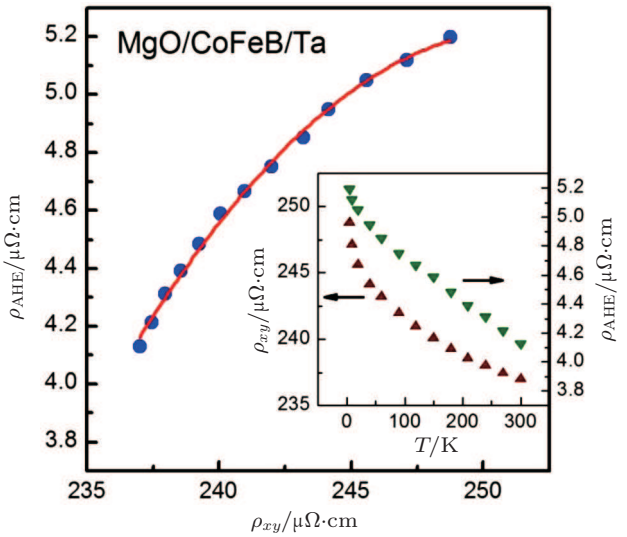


Fig. 8. Representative curves of $\rho_{\rm AHE}$ versus ρ_{xx} for MgO (1.1)/CoFeB (1.22)/Ta (2.2) films ($T_{\rm ann} = 300$ °C). The line is a guide for eyes. Inset shows the temperature dependence of $\rho_{\rm AHE}$ and ρ_{xx}.

Furthermore, the Ta capping layer alone is sufficient to ensure the chemical stability of the samples over time due to the formation of a dense Ta oxide. Although it is hard to accurately determine how thick Ta is oxidized, 1-nm-thick Ta is enough to completely protect the samples.[28] In order to study the thickness of Ta oxide on AHE, two series of samples, Ta (0.55–5)/CoFeB (1.04)/MgO (1.1) and MgO (11)/CoFeB (1.22)/Ta (0.55–5) ($T_{\rm ann} = 300$ °C), were prepared. All the samples show squared loops, indicating 100% out-of-plane remanence. Figure 9 shows the total thickness $(t_{\rm Ta} + t_{\rm CoFeB})$ dependence of $\rho_{\rm AHE}$ for both series of samples. Here, the thickness of Ta in MgO/CoFeB/Ta is reduced by 0.45 nm. The overlap of the two curves suggests that 0.45 nm of Ta thickness should be subtracted from the Ta capping films. Thus, the $\rho_{\rm AHE}$ and ρ_{xx} of the Ta capping film are calculated by subtracting this experimental thickness (0.45 nm) to eliminate the effect of Ta oxide when Ta is capped on the top of a sample.

It is well known that Hall angle is an important parameter for practical applications, because it characterizes the ability of the material to turn the flow of electrons away from the direction of the longitudinal electrical field.[29] Hall angle is defined as $\rho_{\rm AHE}/\rho_{xx}$, which is independent of the measurement accuracy of thickness. Figure 10 shows the Ta thickness dependence of Hall angle $\rho_{\rm AHE}/\rho_{xx}$ for Ta (0.55–5)/ CoFeB (1.04)/MgO (1.1) and MgO (1.1)/CoFeB (1.22)/Ta (0.55–5) films. It is clear that the $\rho_{\rm AHE}/\rho_{xx}$ is similar to that of a traditional Pt-based multilayer. For instance, $\rho_{\rm AHE}/\rho_{xx}$ is 2.2% for Ta (1.1)/CoFeB (1.04)/MgO (1.1) thin film, but $\rho_{\rm AHE}$ and ρ_{xx} are 4.5 and 204 μΩ·cm, respectively, which are much larger than those for a traditional Pt-based multilayer.[14–16] Moreover, $\rho_{\rm AHE}/\rho_{xx}$ increases with the decrease of Ta thickness, which indicates that the thinner Ta layer is much better for device design.

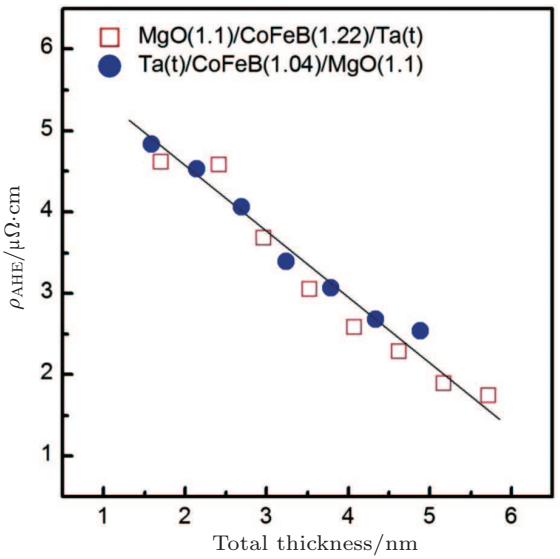


Fig. 9. Total thickness $(t_{\rm Ta} + t_{\rm CoFeB})$ dependence of $\rho_{\rm AHE}$ for both series samples, Ta ($t_{\rm Ta}$)/CoFeB (1.04)/MgO (1.1) and MgO (1.1)/CoFeB (1.22)/Ta ($t_{\rm Ta}$) ($T_{\rm ann} = 300$ °C).

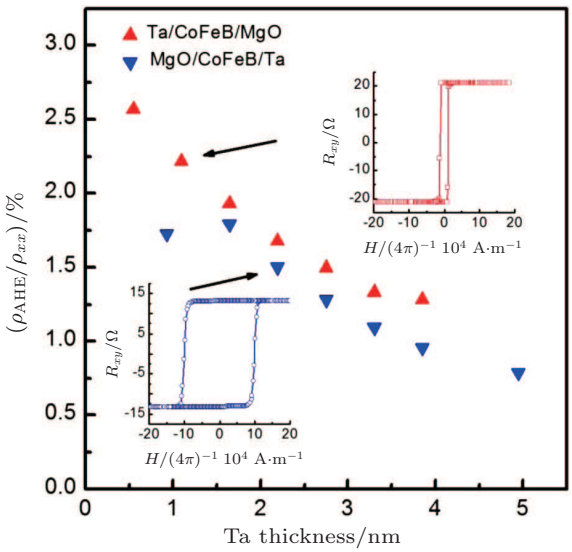


Fig. 10. Ta thickness dependence of Hall angle for both series samples, Ta ($t_{\rm Ta}$)/CoFeB (1.04)/MgO (1.1) and MgO (1.1)/CoFeB (1.22)/Ta ($t_{\rm Ta}$) ($T_{\rm ann} = 300$ °C). The insets show the representative curves of R_{xy} versus H. The red and blue curves are for Ta (1.1)/CoFeB (1.04)/MgO (1.5) and MgO (1.1)/CoFeB (1.22)/Ta (2.2) films, respectively.

4. AHE mechanism in perpendicular CoFeB thin film

There are two mechanisms for AHE.[34–37] One is the intrinsic mechanism, which originates from the spin–orbit coupling in Bloch bands, as identified by Karplus and Luttinger.[34] Recently, the intrinsic mechanism of AHE is believed to be caused by the Berry curvatures over the occupied Bloch states.[37] The other is the extrinsic mechanism, which arises from skew scattering (SS)[35] and side jumps (SJ).[36] Experimentally, a simple scaling relation between ρ_{AHE} and ρ_{xx} is given as

$$\rho_{\mathrm{AHE}} = a\rho_{xx} + b\rho_{xx}^2, \tag{4}$$

where the first term comes from the skew scattering and the second comes from side jumps and the intrinsic Karplus–Luttinger terms.[34] In general, the AHE mechanisms can be directly investigated from the relationship between ρ_{AHE} and ρ_{xx}, if the sample has a high Curie temperature, as Fe does.[38] When the sample has a low Curie temperature, a temperature-dependent factor $f(T)$ should be considered.[39] Recently, we reported that the temperature dependence of magnetization follows the Bloch law, which predicts $M(T) = M_0 - kBT^{3/2}$, where k is a prefactor involved in interlayer coupling and B is the bulk spin-wave stiffness parameter.[21] At 300 K, the saturation magnetization $M_{\mathrm{S}} = 940 \times 10^5$ A/m, which is quite close to a fitting of results from polarized neutron reflectivity.[10]

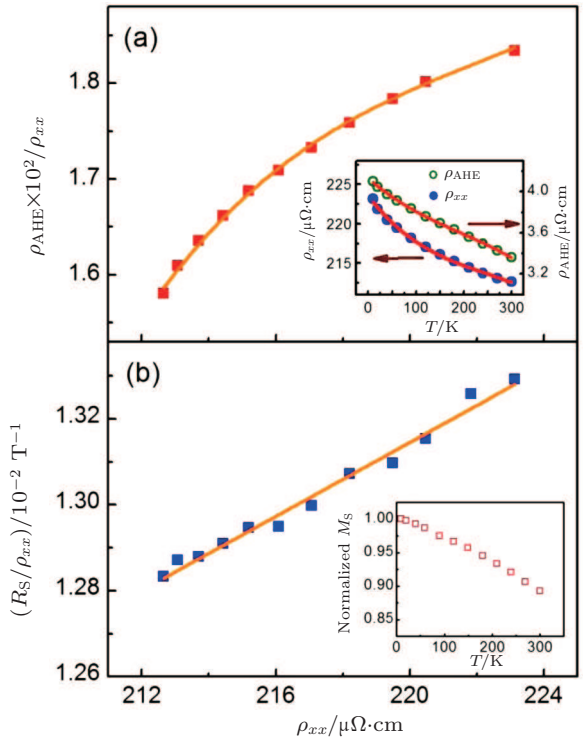


Fig. 11. (a) CoFeB thickness dependence of ρ_{AHE} and ρ_{xx} for MgO (1.1)/CoFeB (t)/Ta (2.2) films ($T_{\mathrm{ann}} = 300$ °C). The inset shows the temperature dependence of ρ_{AHE} and ρ_{xx}. (b) The scaling relation of R_{S} versus ρ_{xx} according to Eq. (1). The inset shows the temperature dependence of magnetization.

Figure 11 shows the curves of $\rho_{\mathrm{AHE}}/\rho_{xx}$ versus ρ_{xx} and R_{S}/ρ_{xx} versus ρ_{xx} ($R_{\mathrm{S}} \approx \rho_{\mathrm{AHE}}/\mu M_{\perp}$) for the Ta(2.2)/CoFeB(1.04)/MgO(5) film. The inset shows the temperature dependence of ρ_{AHE} and ρ_{xx} in the temperature range of 5 K to 300 K. It is clear that the curve of $\rho_{\mathrm{AHE}}/\rho_{xx}$ versus ρ_{xx} is very different from that of R_{S}/ρ_{xx} versus ρ_{xx} because varying M_{S} cannot be neglected. Here, the scaling relation for AHE has been fitted from the curves of R_{S} versus ρ_{xx} to eliminate the temperature-dependent factor. It is found that the absolute magnitude of SJ is about three times as large as that of SS.[21] This is to say, the side jump mechanism dominates the AHE in perpendicular Ta/CoFeB/MgO films. Similar conclusions have been reached for the perpendicular MgO/CoFeB/Ta films. On the other hand, the fitting process is found to be determined by the accuracy of magnetic measurements for quite thin magnetic thin films ($\sim$ 1 nm).

Recently, a unified theory of the AHE mechanism has been proposed based on multiband ferromagnetic metals with dilute impurities.[40,41] According to this unified theory, three regimes can be distinguished as a function of the longitudinal conductivity, σ_{xx}.[40–42] The magnitude of the anomalous Hall conductivity (AHC) is constant in the intrinsic moderately dirty regime ($\sigma_{xx} \sim 10^3$ S/cm) for Fe- and Ni-based dilute alloys.[41] This is in accord with the longitudinal resistivity ρ_{xx} of about 200 μΩ·cm for the perpendicular CoFeB thin film. Based on the relation of $\sigma_{xx} = \rho_{xx}/(\rho_{\mathrm{AHE}}^2 + \rho_{xx}^2)$, the conductivity σ_{xx} of the perpendicular CoFeB thin film (both Ta/CoFeB/MgO and MgO/CoFeB/Ta) is about 5×10^3 S/cm.[21] This is to say, σ_{xx} of the perpendicular CoFeB thin film belongs to the moderately dirty region, although it may be close to the boundary between the moderately dirty and dirty regions of conductivity.[40–42] Hence, it suggests that the AHE in perpendicular CoFeB thin film is dominated by the scattering-independent mechanism, which implies that ρ_{AHE} is proportional to the square of ρ_{xx}. The origin of AHE in the multilayers is not yet understood and is still a major challenge for AHE theory. Our results reveal that the scattering-independent mechanism dominates the origin of AHE in the perpendicular CoFeB thin films.

5. A preliminary AHE application of the perpendicular CoFeB thin film

Among all the applications using PMA, the ferromagnetic thin film with highly sensitive anomalous Hall effect is a candidate for magnetic field sensors, memory, and logic devices.[17] The Hall resistance in a magnetic thin film consists of two terms: one represents the ordinary Hall effect and the other, which is much larger, represents the AHE. Linear Hall field sensitivity (LHFS) is defined as the ratio of anomalous Hall resistance (R_{AH}) to the out-of-plane saturation field (H_{S}), $R_{\mathrm{AH}}/H_{\mathrm{S}}$. Because the H_{S} of a typical magnetic thin film is large ($>$ 1 T), its LHFS is no more than several tens Ω/T, which is much lower than that of of semiconductors (e.g.

1100 Ω/T for the ultra-sensitive InSb[43]). Thus, the conventional Hall sensors for probing magnetic fields are usually made of a semiconductor.[43,44] However, the magnetic thin films exhibit some advantages, such as high operating frequency and low temperature coefficient, in contrast to conventional semiconductors.[13,14] Particularly, due to the strong PMA induced by a noble metal, such as Pt,[13–17] H_S is dramatically reduced in CoFe/Pt multilayers with thick Pt layers to stabilize the interfacial anisotropy,[15,16] so in such cases, large LHFS has been observed. So far, the best reported LHFS is over 1.2×10^4 Ω/T, measured in an FePt granular alloy film with a large amount of Pt.[17] Even though incorporating thick Pt layers in these thin films results in high cost and a longitudinal resistivity that is low enough to frustrate efforts to reduce the size of devices, the magnetic thin films with highly sensitive AHE have gained renewed interest.

Based on the analysis in Section 2, we come to the following scenario for the AHE in a perpendicular CoFeB sandwiched by MgO and Ta, as shown in Fig. 12: At first, the saturation field H_a of the CoFeB/Ta bilayer is reduced, but a perpendicular easy axis cannot be achieved (Fig. 12(a)). And then, the interfacial anisotropy increases further when the MgO layer is introduced (Fig. 12(b)). Finally, a perpendicular CoFeB is obtained. As we mentioned above, the H_C for perpendicular CoFeB is different, due to the difference of the layer deposition sequence. As seen from the insets of Fig. 11, the H_C of Ta (1.1)/CoFeB (1.04)/MgO (1.1) film is only 1 kA/m, whereas the H_C of MgO (1.1)/CoFeB (1.22)/Ta (1.1) film is 8 kA/m. The results are consistent with their effective anisotropy values, i.e., $K_{eff} = 2.4 \times 10^4$ J/m and 4×10^4 J/m for Ta/CoFeB/MgO and MgO/CoFeB/Ta, respectively. Thus, the smaller H_C of the Ta/CoFeB/MgO films is due to its lower K_{eff}, which is an advantage for practical applications.

On the other hand, *ab initio* calculation reveals that the interfacial anisotropy at the interface of CoFeB/MgO can be tuned by the crystallization of the thick MgO layer.[27] Thus, large linear AHE is achieved by increasing the thickness of the MgO layer in MgO/CoFeB/Ta thin films. Unlike the thick Pt layer in the traditional Pt-based multilayer which is used to stabilize PMA. Ta layer in the MgO/CoFeB/Ta thin film is independent of the mechanism of interfacial PMA. The main effect of the Ta layer in MgO/CoFeB/Ta thin film is to absorb boron during the annealing process. Hence, to reach a giant LHFS, we can adjust K_{eff} by tuning MgO thickness and then increase R_{AH} further by reducing the thickness of the Ta.[31] Figure 13 shows the trend of LHFS for ferromagnetic materials. The highest LHFS at room temperature is 23760 Ω/T when $t_{Ta} = 0.7$ nm, which is 21 times larger than that of the best semiconductor (1100 Ω/T for InSb). It is clear that the out-of-plane magnetization saturation field and then the switching field can be tuned by adjusting the interfacial anisotropy. Therefore, a large AHE signal, a large longitudinal resistivity, and a low switching field have been obtained simultaneously in these perpendicular MgO/CoFeB/Ta trilayers.

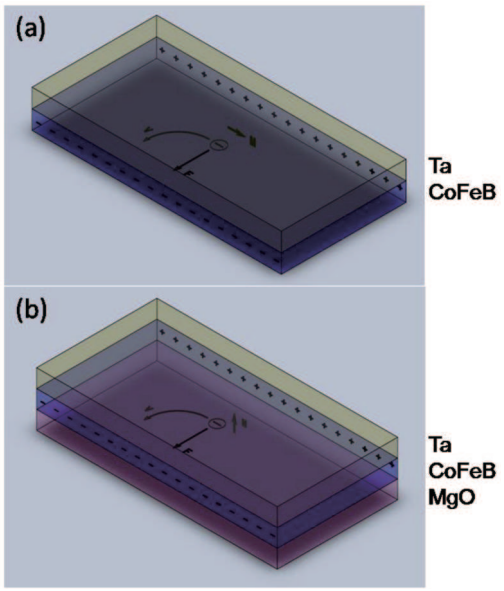


Fig. 12. Schematics of the anomalous Hall effects in (a) an in-plane CoFeB/Ta bilayer and (b) a perpendicular MgO/CoFeB/Ta trilayer.

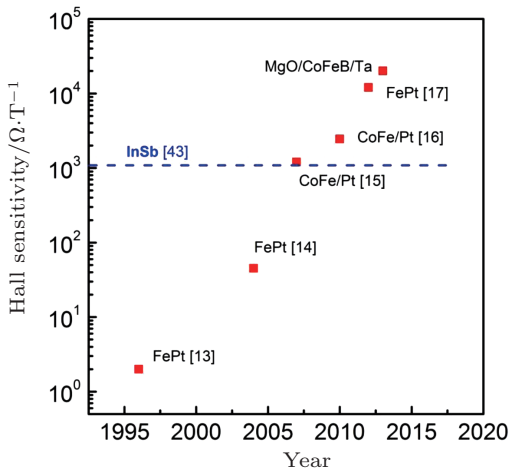


Fig. 13. The trend of LHFS discoveries in ferromagnetic materials. The numbers next to data points are the reference numbers for this paper.

6. Conclusion

In conclusion, we have summarized our recent achievements in PMA properties of the CoFeB sandwiched by MgO and tantalum layers. We found that there is no strong relationship between PMA and the thickness of the tantalum or MgO cap layer. The large PMA is related to the low magnetization of CoFeB deposited on MgO. Typical perpendicular anisotropies are 2.4 J/m for Ta/CoFeB/MgO thin film and 4×10^4 J/m for MgO/CoFeB/Ta.

We also demonstrated a large anomalous Hall effect in perpendicular CoFeB thin film. The optimized ρ_{AHE} and ρ_{xx} can reach as high as 4.5 μΩ·cm and 204 μΩ·cm, respectively,

in the Ta (1.1)/CoFeB (1.04)/MgO (1.1) film. Its Hall angle is 2.2% whereas its coercivity field is only 1 kA/m. Moreover, the MgO/CoFeB/Ta thin film with a thick MgO layer is sensitive to the applied field. Our results show that a large anomalous Hall resistivity, a large longitudinal resistivity, and a low switching field can be achieved simultaneously in perpendicular CoFeB thin film, making it a candidate for use in practical devices.

Acknowledgments

The authors would like to thank Dr. Wu S. B. for some magnetotransport measurements and Chen B. and Prof. Liu B. G. for the discussion of *ab initio* calculation. A portion of this work is based on the data obtained at 1W1A, BSRF. The author gratefully acknowledges the assistance of scientists of the Diffuse X-ray Scattering Station during the experiments.

References

[1] Stiles M D 2005 *Ultrathin Magnetic Structures III*, ed. Heinrich B and Bland J A C (New York: Springer)
[2] Moser A, Takano K, Margulies D T, Albrecht M, Sonobe Y, Ikeda Y, Sun S H and Fullerton E E 2002 *J. Phys. D: Appl. Phys.* **35** R157
[3] Kent A D 2010 *Nat. Mater.* **9** 699
[4] Johnsony M T, Bloemenzx P J H, den Broedery F J A and de Vriesz J J 1996 *Rep. Prog. Phys.* **59** 1409
[5] Jung J H, Lim S H and Lee S R 2010 *Appl. Phys. Lett.* **96** 042503
[6] de Person P, Warin P, Jamet M, Beigne C and Samson Y 2007 *Phys. Rev. B* **76** 184402
[7] Ikeda S, Miura K, Yamamoto H, Mizunuma K, Gan H D, Endo M, Kanai S, Hayakawa J, Matsukura F and Ohno H 2010 *Nat. Mater.* **9** 721
[8] Endo M, Kanai S, Ikeda S, Matsukura F and Ohno H 2010 *Appl. Phys. Lett.* **96** 212503
[9] Worledge D C, Hu G, Abraham D W, Sun J Z, Trouilloud P L, Nowak J, Brown S, Gaidis M C, O'Sullivan E J and Robertazzi R P 2011 *Appl. Phys. Lett.* **98** 022501
[10] Zhu T, Yang Y, Yu R C, Ambaye H, Lauter V and Xiao J Q 2012 *Appl. Phys. Lett.* **100** 202406
[11] Monso S, Rodmacq B, Auffret S, Casali G, Fettar F, Gilles B, Dieny B and Boyer P 2002 *Appl. Phys. Lett.* **80** 4157
[12] Gerber A 2007 *J. Magn. Magn. Mater.* **310** 2749
[13] Canedy C L, Gong G Q, Wang J Q and Xiao G 1996 *J. Appl. Phys.* **79** 6126
[14] Miao G X and Xiao G 2004 *Appl. Phys. Lett.* **85** 73
[15] Zhu Y and Cai J W 2007 *Appl. Phys. Lett.* **90** 012104
[16] Zhang S L, Teng J, Zhang J Y, Liu Y, Li J W, Yu G H and Wang S G 2010 *Appl. Phys. Lett.* **97** 222504
[17] Lu Y M, Cai J W, Pan H Y and Sun L 2012 *Appl. Phys. Lett.* **100** 022404
[18] Yakata S, Kubota H, Suzuki Y, Yakushiji K, Fukushima A, Yuasa S and Ando K 2009 *J. Appl. Phys.* **105** 07D131
[19] Kubota H, Ishibashi S, Saruya T, Nozaki T, Fukushima A, Yakushiji K, Ando K, Suzuki Y and Yuasa S 2012 *J. Appl. Phys.* **111** 07C723
[20] Yamanouchi M, Koizumi R, Ikeda S, Sato H, Mizunuma K, Miura K, Gan H D, Matsukura F and Ohno H 2011 *J. Appl. Phys.* **109** 07C712
[21] Wu S B, Zhu T, Yang X F and Chen S 2013 *J. Appl. Phys.* **113** 17C716
[22] Lauter V Ambaye H, Goyette R, Lee W H and Parizzi A 2009 *Physica B* **404** 2543
[23] Ankner J F and Felcher G P 1999 *J. Magn. Magn. Mater.* **200** 741
[24] Ding Y F, Judy J H and Wang J P 2005 *J. Appl. Phys.* **97** 10J117
[25] Johnsony M T, Bloemenzx P J H, den Broedery F J A and de Vriesz J J 1996 *Rep. Prog. Phys.* **59** 1409, and references therein
[26] Yang H X, Chshiev M, Dieny B, Lee J H, Manchon A and Shin K H 2011 *Phys. Rev. B* **84** 054401
[27] Zhu T, Chen B, Zhang Q H, Yu R C and Liu B G (unpublished)
[28] Mizuguchi T and Kano H 2001 *IEEE Trans. Magn.* **37** 1742
[29] Moritz J, Rodmacq B, Auffret S and Dieny B 2008 *J. Phys. D: Appl. Phys.* **41** 135001
[30] Pakhomov A B, Yan X and Zhao B 1995 *Appl. Phys. Lett.* **67** 3497
[31] Zhu T, Yang Y and Yu R C (unpublished)
[32] Feldman B and Dunham S T 2009 *Appl. Phys. Lett.* **95** 222101
[33] Jen S U, Yao Y D, Chen Y T, Wu J M, Lee C C, Tsai T L and Chang Y C 2006 *J. Appl. Phys.* **99** 053701
[34] Karplus R and Luttinger J M 1954 *Phys. Rev.* **95** 1154
[35] Smit J 1958 *Physica* **24** 39
[36] Berger L 1970 *Phys. Rev. B* **2** 4559
[37] Yao Y G, Kleinman L, Macdonald A H, Sinova J, Jungwirth T, Wang D S, Wang E and Niu Q 2004 *Phys. Rev. Lett.* **92** 037204
[38] Tian Y, Ye L and Jin X F 2009 *Phys. Rev. Lett.* **103** 087206
[39] Chen M, Shi Z, Xu W J, Zhang X X, Du J and Zhou S M 2011 *Appl. Phys. Lett.* **98** 082503
[40] Onoda S, Sugimoto N and Nagaosa N 2006 *Phys. Rev. Lett.* **97** 126602
[41] Nagaosa N, Sinova J, Onoda S, MacDonald A and Ong N P 2010 *Rev. Mod. Phys.* **82** 1539
[42] Sangiao S, Morellon L, Simon G, de Teresa J M, Pardo J A, Arbiol J and Ibarra M R 2009 *Phys. Rev. B* **79** 014431
[43] Michele L D, Shelly C, de Marco P, See P, Cox D and Kazakova O 2011 *J. Appl. Phys.* **110** 063916
[44] Manandhar P, Chen K S, Aledealat K, Mihajlović G, Yun C S, Field M, Sullivan G J, Strouse G F, Chase P B, von Molnár S and Xiong P 2009 *Nanotechnology* **20** 355501